

Massive stars reveal variations of the stellar initial mass function in the Milky Way stellar clusters

Sami Dib^{1*}, Stefan Schmeja^{2,3}, Sacha Hony⁴

¹Niels Bohr Institute & Centre for Star and Planet Formation, University of Copenhagen, Øster Voldgade 5-7, DK-1350, Copenhagen, Denmark.

²Astronomisches Rechen-Institut, Zentrum für Astronomie der Universität Heidelberg, Mönchhofstraße. 12-14, 69120 Heidelberg, Germany.

³Technische Informationsbibliothek, Welfengarten 1b, 30167 Hannover, Germany

⁴Institut für Theoretische Astrophysik, Zentrum für Astronomie der Universität Heidelberg, Albert-Überle-Straße 2, 69120 Heidelberg, Germany.

4 January 2019

ABSTRACT

We investigate whether the stellar initial mass function (IMF) is universal, or whether there are significant cluster-to-cluster variations of the IMF among young stellar clusters in the Milky Way. We propose a method to uncover the range of variation of the parameters that describe the IMF for the population of young clusters in the Milky Way. The method relies exclusively on the high mass content of the clusters, but is able to yield information on the distributions of parameters of the IMF over the entire stellar mass range. This is achieved by appropriately comparing the fractions of single and lonely massive O stars in a recent catalog of the Milky Way clusters with a large library of simulated clusters built with various distribution functions of the IMF parameters. The masses of synthetic clusters are randomly drawn using a power-law distributions function, while stellar masses in the clusters are randomly drawn using a tapered power-law function. The synthetic clusters are further corrected for the effects of binary population, stellar evolution, sample incompleteness, and estimates are made for the effects of ejected O stars. Our findings indicate that broad distributions of the IMF parameters are required in order to reproduce the fractions of single and lonely O stars in the Milky Way clusters and they do not lend support to the existence of a cluster mass-maximum stellar mass relation. We propose a probabilistic formulation of the IMF based on the distribution functions of its parameters.

Key words: galaxies: star clusters - Turbulence - ISM: clouds - open clusters and associations

1 INTRODUCTION

The initial mass function (IMF) of stars in the Galaxy (i.e., the distribution of the masses of stars at their birth), is of fundamental importance for astrophysics. The IMF controls the efficiency of star formation in molecular clouds (e.g., Zinnecker & Yorke 2007; Dib et al. 2011; 2013), the size distribution of protoplanetary disks in stellar clusters (e.g., Vincke et al. 2015), the radiative and mechanical feedback from stars into the interstellar medium (e.g., Dib et al. 2006; Martizzi et al. 2016) and the dynamical and chemical evolution of galaxies (e.g., Boissier & Prantzos 1999). In the Milky Way, as in other galaxies, stars form mostly, if not exclusively, in clusters and associations (e.g., Carpenter 2000, Lada & Lada 2003). As clusters age, the expulsion of gas by

stellar feedback as well as dynamical interactions between stars and binary systems in the cluster soften its gravitational potential, leading to its expansion and to its partial or total dissolution into the field of the galaxy (e.g., Goodwin & Bastian 2006; Pfalzner & Kaczmarek 2013). The mass function of stars in the field of a galaxy is thus the convolution of the galaxy’s cluster formation history with the stars from dissolved clusters and the stars that have been ejected from surviving clusters. In our Galaxy, the present day stellar mass function, uncorrected for the binary population, rises from the brown dwarf and low stellar mass regime until it peaks at $\approx 0.3 - 0.5 M_{\odot}$ after which it declines steeply in the intermediate-to-high mass regime (e.g., Miller & Scalo 1979; Scalo 1986; Kroupa 1993; Chabrier 2003; Bochanski et al. 2010; Rybizki & Just 2015). Several distribution functions are used to describe its shape, such as a multi-component power-law (Kroupa 2001), a lognormal coupled to a power-

* E-mail: sami.dib@gmail.com; sdib@nbi.dk

law beyond $1 M_{\odot}$ (Chabrier 2005), a tapered power law (de Marchi 2010; Parravano et al. 2011), an order-3 Logistic function (Maschberger 2013), or a modified lognormal (Basu et al. 2015).

An outstanding question is whether there are significant variations in the shape of the IMF among stellar clusters in the Milky Way and how well the IMF of each cluster resembles the mass function of stars in the Galaxy (e.g., Elmegreen 2004; Scalo 2005; Dib 2014a). Stars in young clusters have roughly the same age, metallicity, and are located at the same distance. Thus, one can presume that their observed present day mass functions (PDMFs¹) are a fair representation of their IMFs. Probing the universality of the IMF among stellar clusters in the Milky Way and in other galaxies is one of the most challenging issues in modern astrophysics. For a Galactic star formation rate (SFR) between 0.5 and $1.5 M_{\odot} \text{ yr}^{-1}$, the Galaxy is expected to form a few tens to a few hundred thousands of clusters in a period of $\sim 10 - 12$ Myrs². The IMF has been derived in the Galaxy and in the Magellanic Clouds by many groups for a small fraction of this total number and usually for individual young clusters and associations as well as for more evolved open clusters (e.g., Massey et al. 1998; Preibisch et al. 2002; Liu et al. 2003; Luhman 2004, 2007; Moraux et al. 2004; Selman & Melnick 2005; Bouvier et al. 2008; Liu et al. 2009; Sung & Bessel 2010; Ojha et al. 2010; Delgado et al. 2011; Gennaro et al. 2011; Lodieu et al. 2011; Alves de Oliveira et al. 2012; Mallick et al. 2014; among many others). The comparison of the parameters that describe the shape of the IMF between these works is not straight forward. Observations of stellar clusters have been carried out using different telescopes with different sensitivities, and different methods are employed to reduce the data and to correct for the effects of extinction and stellar incompleteness. The conversion of measured stellar fluxes into masses is also performed using different stellar evolutionary tracks (see interesting discussions in Scalo 1998 and Massey 2011). Based on the comparison of a relatively small number of clusters compiled from these observations, there are claims that within the uncertainties, the shape of the IMF of some clusters are similar, at least in the intermediate to high-mass stellar regime (e.g., Bastian et al. 2010; Offner et al. 2014). However, there are also a few other studies in which the parameters of the IMF have been derived using a more homogeneous approach and that show significant cluster-to-cluster variations (e.g., Sharma et al. 2008; Massey 2011; Scholz et al. 2013; Dib et al. 2014a; Lim et al. 2015; Weisz 2015). In principle, a direct assessment of the universality of the IMF could be achieved by constructing the IMF for a large number of Galactic and extragalactic young clusters across the entire stellar mass range. This is however beyond the reach of current observational programs. Surveys that contain a large number of clusters such as the PHAT survey of the Andromeda galaxy (85 clusters)

are sensitive only to the intermediate-to-high mass stellar content of the clusters (stars with masses $M_{*} \geq 2 M_{\odot}$) and thus can only make statements about the IMF in this mass regime (Weisz et al. 2015). As in the case of Galactic clusters (e.g., Sharma et al. 2008; Dib 2014a), the findings of Weisz et al. (2015) indicate values of the slope of the IMF in the intermediate-to-high mass regime that do not overlap within the 1σ confidence intervals (see Figure 4 in their paper), and that are, for many of them, not compatible with the values of the parameters for the Galactic field stellar mass function.

In this paper, we propose an alternative method to uncover the range of variation of the parameters that describe the IMF for the populations of young clusters ($\lesssim 12$ Myrs) in the Milky Way. The method is based on the fact that the number statistics of massive stars in Galactic clusters is very sensitive to the underlying distribution of the IMF parameters in the clusters. The method relies exclusively on the high mass content of the clusters, but is able to yield information on the distributions of parameters of the IMF over the entire stellar mass range. This is achieved by appropriately comparing the fractions of single and lonely O stars in a recent catalog of the Milky Way clusters (the MWSC catalog; Schmeja et al. 2014) with a very large library of simulated clusters built with various distribution functions of the IMF parameters. The simulated synthetic clusters include corrections for the binary population, stellar evolution and sample incompleteness. In §. 2, we discuss the essential aspects of the method that is employed to compare models and observations and in §. 3, we briefly present the observational data. The models of synthetic clusters are presented in §. 4, and the comparison to the observation is performed in §. 5. In §. 6 we compare our approach to previous work on closely related topics and in §. 7 we discuss our results in connection to the physical processes that may lead to variations of the IMF. Finally, we present our conclusions in §. 8.

2 METHOD

The number statistics of massive stars in clusters is very sensitive to the underlying distribution of the IMF parameters among Galactic clusters. In this work, we want to make use of the massive stellar population in young Galactic stellar clusters in order to infer the distribution of the parameters that describe the shape of the IMF across the entire stellar mass range. This can be achieved by comparing the fractions of single and lonely massive O stars in a recent catalog of the Milky Way clusters (the MWSC catalog; Schmeja et al. 2014) with a very large library of simulated clusters built with various distribution functions of the IMF parameters. Since in the simulated clusters, we are populating their system IMFs, a star as defined in this work could be an individual star or a binary system. Thus, an O star in the cluster could be a single star or one/both components of a binary system with a mass that is $\geq 15 M_{\odot}$. An O star in a cluster is called "single" if it is the only star, or a binary system with any of its components, that has a mass $\geq 15 M_{\odot}$ in

¹ In the remainder of the paper, we will refer to the PDMF, especially to that of young clusters as being the IMF. However, it should always be kept in mind that we are dealing here with PDMFs.

² The exact numbers depend primarily on the SFR, the exponent of the initial cluster mass function (ICLMF), and the lower and upper mass cutoffs of the ICLMF. See §. A for more quantitative estimates

the cluster. The fraction of single O stars³ in a population of clusters is thus given by:

$$f_{single} = \frac{N_{O,single}}{N_O}, \quad (1)$$

where $N_{O,single}$ is the total number of single O stars and N_O is the total number of O stars in all clusters. We also measure the fraction of "lonely" O stars in the clusters. A lonely O star in a cluster is a single O star with the additional constraint that the next massive system in the cluster is less massive than $10 M_\odot$ (i.e., absence of high mass B stars with masses between 10 and $15 M_\odot$). The fraction of lonely O stars is given by:

$$f_{lonely} = \frac{N_{O,lonely}}{N_O}, \quad (2)$$

where $N_{O,lonely}$ is the total number of lonely stars in the clusters. The basic idea of the method relies on the comparison of $f_{O,single}$ and $f_{O,lonely}$ measured for a recent catalogue of stellar clusters in the Milky Way with those derived for populations of stellar clusters that are generated with various prior functions for the distributions of the IMF parameters. A number of important corrections have to be applied to the zero-age synthetic clusters and to their stellar content before they can be compared to the observations. The description of the observational sample of clusters is given in §. 3, while the synthetic models of clusters are described in §. 4.

3 OBSERVATIONAL CATALOG OF CLUSTERS

The observations used in this paper come from the Milky Way Stellar Clusters survey (MWSC) (Kharchenko et al. 2012; Kharchenko et al. 2013; Schmeja et al. 2014)⁴, which lists ~ 3200 clusters with ages between ~ 1 Myr and ~ 7 Gyr. The clusters are detected as density and velocity enhancements in the Two Micron All Sky Survey (2MASS) (Skrutskie et al. 2006) and the proper motions PPMXL survey (Röser et al. 2010). The survey includes clusters up to a distance of ~ 10 kpc from the position of the Sun but most clusters lie within a distance $\lesssim 1.8$ kpc. The files in the catalog list the B, V, and J, H, K magnitudes of each star in each cluster present in the catalog, along with other properties such as position, age, cluster membership probability, proper motions, and, when available, the spectral type. The resolved stellar content of each cluster are however not corrected for the effects of the binary population. In this work, we are interested in clusters that could, based on their age, harbor high-mass stars ($M_* \geq 15 M_\odot$), which implies clusters younger than $\tau_{15} \approx 12.3$ Myrs, where τ_{15} is the duration of the Hydrogen and Helium burning phases for a star with a mass of $15 M_\odot$ (Ekström et al. 2012). This brings down the number of clusters useful for our purposes in the MWSC to

$N_{MWSC,cl} = 102$. The individual stellar masses are estimated from the relation between $\log M_*$ and the absolute visual magnitude M_V given by Schilbach et al. (2006). The absolute magnitude M_V is computed from the apparent magnitude m_V , the distance, and the extinction E_{B-V} which are all listed in the MWSC (Kharchenko et al 2013). The fraction of single and lonely O star in the MWSC catalog measured using Eq. 1 and Eq. 2 are $f_{single,O}(MWSC) = 12.4\%$ and $f_{lonely,O}(MWSC) = 6.5\%$.

4 MODELS

4.1 Generating populations of zero-age clusters

The possibility of detecting massive O stars in the Galaxy is bound by the relatively short lifetime of these stars and by the value of the Galactic star formation rate (SFR). The models of stellar clusters that are compared to the observations are generated in the following way: assuming that all stars form in clusters, the total mass contained in the young population of Galactic stellar clusters that are likely, based on their age, to contain O stars ($M_* \geq 15 M_\odot$) is given by:

$$\Sigma_{cl} = \int_0^{\tau_{15}} \text{SFR}(t) \times dt, \quad (3)$$

where $\text{SFR}(t)$ is the time dependent star formation rate over the last τ_{15} timescale of the lifetime of the Galaxy. The Galactic SFR over such a relatively short period of time can be assumed to be constant and Σ_{cl} can be approximated by $\Sigma_{cl} \approx \text{SFR} \times \tau_{15}$. We consider three values of the Galactic SFR of 0.68 , 1 , and $1.45 M_\odot \text{ yr}^{-1}$ that are the lower, central, and upper estimates obtained from the count of young stellar objects in the GLIMPSE survey of the Galactic plane (Robitaille & Whitney 2010). The individual cluster masses are stochastically sampled from the mass reservoir Σ_{cl} using an initial cluster mass function (i.e., the mass function of clusters at their birth, ICLMF). The ICLMF is taken to be a power-law, between the minimum and maximum cluster masses of $M_{cl,min}$ and $M_{cl,max}$, and is given by:

$$\frac{dN_{cl}}{dM_{cl}} = A_{cl} \times M_{cl}^{-\beta}, \quad (4)$$

where A_{cl} is the normalization constant given by:

$$\int_{M_{cl,min}}^{M_{cl,max}} A_{cl} \times M_{cl}^{-\beta+1} dM_{cl} = \Sigma_{cl}. \quad (5)$$

We fix $M_{cl,max}$ at $5 \times 10^4 M_\odot$ which is the mass of the most massive clusters in the Milky Way (e.g., Figer et al. 1999; Dib et al. 2007; Ascenso et al. 2007; Harayama et al. 2008; Clark et al. 2009) and explore values of $M_{cl,min} = 50$ (fiducial), 20 , and $10 M_\odot$. Our fiducial value of β is 2 as this is in agreement with the slope of the cluster mass function at intermediate- to high cluster masses in nearby galaxies (e.g., Elmegreen & Efremov 1997; Zhang & Fall 1999; Hunter et al. 2005; de Grijs & Anders 2006; Selman & Melnick 2008; Larsen 2009; Chandar et al. 2010; Fall & Chandar 2012) and with theoretical expectations (Elmegreen 2006; Dib et al. 2011; Dib 2011; Dib et al. 2013). We also consider cases with $\beta = 2.2$ and $\beta = 1.8$. For each cluster with an assigned

³ For simplicity, we will use the term "star" to define both individual stars or binary systems

⁴ The full list of cluster parameters is available at the CDS via anonymous ftp to cdsarc.u-strasbg.fr (130.79.128.5) or via <http://cdsarc.u-strasbg.fr/viz-bin/qcat?J/A+A/568/A51>

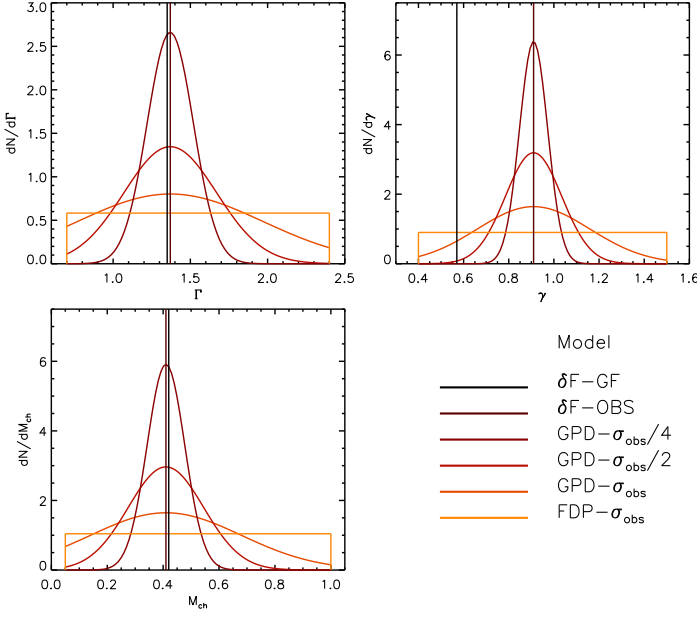


Figure 1. The figure displays the probability distribution functions of the three parameters that describe the IMF used in this work. The acronym δF -GF refers to delta functions of the parameters at the positions of the Galactic field values, whereas δF -OBS refers to delta functions located at the mean values of the parameters derived by Dib (2014a) for a sample of 8 young Galactic stellar clusters. The cases $GPD-\sigma_{obs}$, $GPD-\sigma_{obs}/2$, and $GPD-\sigma_{obs}/4$ correspond to cases with a Gaussian probability distribution of the IMF parameters whose half-width is related to 1, 0.5, and 0.25 the values of the dispersion of each parameter in the sample of Dib (2014a). $FDP-\sigma_{obs}$ corresponds to a case where the probability distribution function of each parameter is given by a boxcar function whose width is given by $2\sigma_{obs}$. The lower and upper truncations for each of the parameters correspond to the lower and upper limits of these parameters derived by Dib (2014a).

mass M_{cl} , the masses of star-systems (i.e., individual stars or binary systems) in the clusters are randomly sampled using a tapered power law (TPL) distribution function (Parravano et al. 2011). Without any assigned binary fraction, a stellar “system” of mass M_* can correspond to an individual star or to a binary system. The TPL function is given by

$$\frac{dN_*}{d\log M_*} = A_* \times M_*^{-\Gamma} \left\{ 1 - \exp \left[- \left(\frac{M_*}{M_{ch}} \right)^{\gamma+\Gamma} \right] \right\}, \quad (6)$$

where dN_* is the number of stellar systems with the logarithm of their masses between $\log M_*$ and $\log M_* + d\log M_*$, and A_* is the normalization coefficient which is given by:

$$\int_{M_{*,min}}^{M_{*,max}} A_* \times M_*^{-\Gamma+1} \left\{ 1 - \exp \left[- \left(\frac{M_*}{M_{ch}} \right)^{\gamma+\Gamma} \right] \right\} dM_* = M_{cl}. \quad (7)$$

The TPL function describes the IMF with only three parameters, the slope in the low mass regime (γ), the slope in the intermediate-to-high mass regime (Γ), and the characteristic mass (M_{ch}). The minimum stellar mass, $M_{*,min}$, is always taken to be $0.02 M_\odot$. The maximum stellar mass,

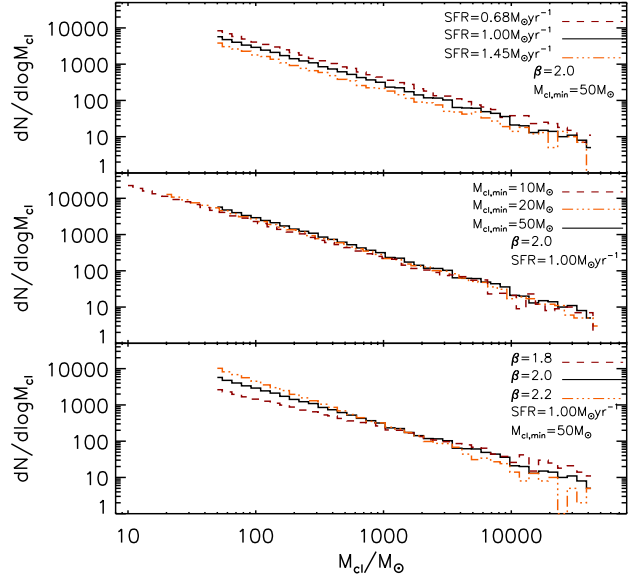


Figure 2. The initial cluster mass function (ICLMF) for various values of its parameters. Several realizations of the ICLMF with various values of the star formation rate (top panel), the minimum cluster mass ($M_{cl,min}$), and the exponent of the power-law function that describes the ICLMF (β). The logarithmic bin size is $\log(M_{cl}/M_\odot) = 0.075$.

$M_{*,max}$, is either given by $\min[M_{cl}, 150 M_\odot]$ (corresponding to the case of stochastic sampling) or is dictated by a cluster mass-maximum stellar mass relation ($M_{cl} - M_{*,max}$) relation proposed by Weidner & Kroupa (2004). We test models in which the distributions of the parameters (γ , Γ , M_{ch}) are either given by delta function (all clusters have the same value of the parameters), Gaussian functions, or boxcar functions. A recent study found that the mean values of the parameters among a relatively small sample of young Galactic stellar clusters are $\Gamma_{obs} = 1.37$, $\gamma_{obs} = 0.91$ and $M_{ch,obs} = 0.41 M_\odot$ with standard deviations of $\sigma_{\Gamma_{obs}} = 0.60$, $\sigma_{\gamma_{obs}} = 0.25$, and $\sigma_{M_{ch,obs}} = 0.27 M_\odot$, respectively (Dib 2014a). When drawing the parameters from Gaussian distributions, the distributions are always centered on these observed mean values. We test dispersions of the Gaussian distributions of $(\sigma_{\Gamma_{obs}}, \sigma_{\gamma_{obs}}, \sigma_{M_{ch}})$, $(\sigma_{\Gamma_{obs}}, \sigma_{\gamma_{obs}}, \sigma_{M_{ch}})/2$, and $(\sigma_{\Gamma_{obs}}, \sigma_{\gamma_{obs}}, \sigma_{M_{ch}})/4$, and apply lower and upper cut-offs of (0.4, 1.5) for γ , (0.70, 2.4) for Γ , and (0.05, 1) M_\odot for M_{ch} , which correspond to the lower and upper limits derived by Dib (2014a). These models are labeled $GPD-\sigma/i$ (for Gaussian Probability Distributions, where $i=1, 2$, or 4). They are contrasted with other models in which the distributions of the IMF parameters are delta functions that are either located at the values of the parameters derived by Dib (2014a), or the Galactic field values that are given by $\Gamma_{field} = 1.35$, $\gamma_{field} = 0.57$, and $M_{ch,field} = 0.42 M_\odot$ (Parravano et al. 2011). These families of models are labeled δF -OBS and δF -GF (Delta Function Observations and- Galactic Field, respectively). We also test flat probability distributions (FPD). These are described by boxcar functions between (0.4, 1.5) for γ , (0.7, 2.4) for Γ , and (0.05, 1) M_\odot for M_{ch} . The distribution functions of the parameters of the IMF for all of these models are displayed in Fig. 1.

Fig. 2 displays a few examples of the generated ICLMFs with various permutations of the Galactic SFR, the expo-

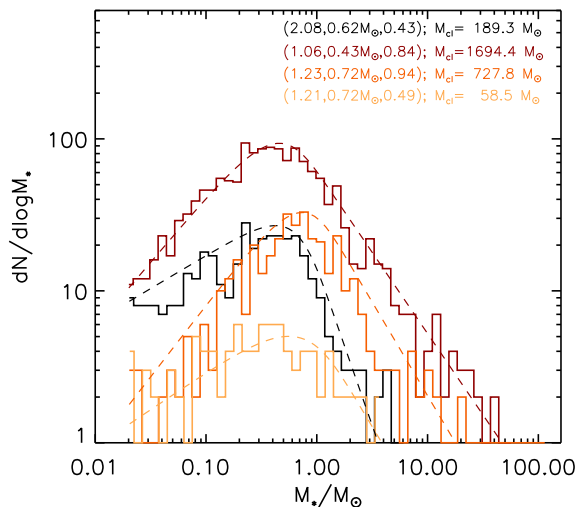


Figure 3. Realizations of the initial stellar mass function (IMF), with different permutations of its parameters (Γ, M_{ch}, γ). The figure displays the shape of the IMF for four permutations of its parameters that are drawn from broad distributions (here from one of the realizations with the GPD- σ_{obs} parameter distributions). The inset displays the set of parameters (Γ, M_{ch}, γ) of the selected clusters, followed by the clusters mass. The logarithmic bin size is $\log(M_{cl}/M_{\odot}) = 0.075$. The dashed lines are over-plots to the generated data of the continuous form of the IMF generated with the corresponding set of parameters.

nent of the ICLMF (β), and the lower mass cutoff in cluster masses ($M_{cl,min}$), and Fig. 3 displays the system IMFs for a few selected clusters drawn from one of the realization of the ICLMF in the GPD- σ_{obs} family of models (i.e., with varying IMFs). Additional technical details on the sampling of the ICLMF and of the IMF are presented in App. §. A.

4.2 Assigning ages to simulated clusters

The synthetic clusters that are generated for each realization of the ICLMF are initially zero-age clusters. Before the stellar populations of the clusters can be corrected for the binary fraction and stellar evolution and then compared with the clusters of the MWSC survey, the clusters have to be assigned ages that are compatible with the observed age distribution of the clusters in the MWSC catalog. Fig. 4 displays the age distribution of the young clusters (with ages $\tau_{cl} < 15$ Myrs) in the MWSC catalog. These ages were computed by Kharchenko et al. (2012) using the Padova web-server CMD2.2⁵, based on the Marigo et al. (2008) calculations for an adopted metallicity of $Z = 0.019$. The figure shows that, to first order, the age distribution is flat, not withstanding the gap at ≈ 1 Myr, as it is particularly difficult to assign ages to very young embedded clusters. There is also no fundamental reason to believe that the SFR and cluster formation rate of the Galaxy would significantly vary over a period of ≈ 15 Myrs, which is the timescale of interest here. Therefore, the synthetic clusters in our models are assigned

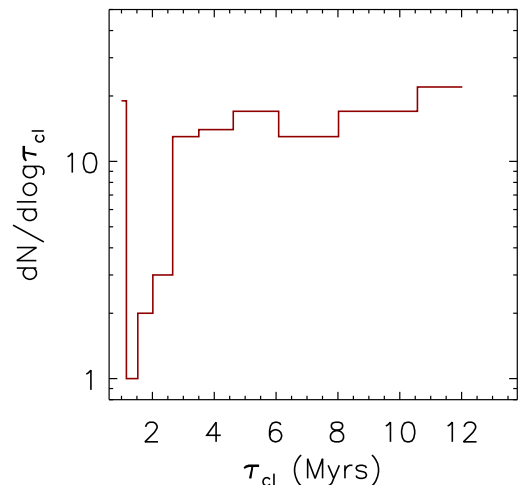


Figure 4. The age distribution of young clusters in the MWSC catalog. The bins in clusters ages, τ_{cl} , are logarithmic with a bin size of $\log(\tau_{cl}(\text{Myrs})) = 0.12$. However, the number distribution of cluster ages is relatively insensitive to the choice of the bin size. Cluster ages have been derived using the isochrones based of the Padova stellar evolutionary tracks (Girardi et al. 2002). To first order, the number distribution of cluster ages in the MWSC can be assumed to be flat.

ages between 0 and $\tau_{15} = 12.3$ Myrs that are randomly drawn from a flat probability distribution function.

4.3 Correcting for the effects of binary population and stellar evolution

In order to properly count the numbers of O stars in the clusters (whether single, lonely, or neither), we have to account for the effect of stellar evolution. O stars whose Hydrogen+Helium burning phases are shorter than the assigned age of their parent cluster would have transformed to stellar remnants (i.e., stellar black holes) and are thus removed from the statistics. The correction for the effects of stellar evolution must be preceded by a correction due to the binary population in the clusters. For each star (i.e., a star-system) with a mass $M_* \geq 2 M_{\odot}$, we assign a binarity probability that is based on the observed binary fraction measured for a large number of systems in the Galaxy (Chini et al. 2012). For star-systems with masses $\geq 15 M_{\odot}$, we assign a binary probability of $P_{bin} = 0.82$ which is the mean of the binary fractions for stars with $\geq 15 M_{\odot}$, whereas for star-systems in the mass range $2 M_{\odot} \leq M_* \leq 15 M_{\odot}$, the binary probability decreases linearly with decreasing mass (Chini et al. 2012). The fit to the observational data in this mass regime is given by $P_{bin} = 0.047 M_* + 0.052$.

The mass ratios of the secondary to the primary stars ($q = M_2/M_1$) in massive binary systems ($\geq 15 M_{\odot}$) are randomly drawn from a flat probability distribution following most up to date observational evidence in massive star forming regions such as the Cygnus OB2 associations (Kobulnicky et al. 2014). For binary systems in the B-type stars mass range ($2 \leq M_*/M_{\odot} \leq 15$), the mass ratios are drawn

⁵ <http://stev.oapd.inaf.it/cgi-bin/cmd>

from a mass-ratio distribution that is slightly peaked towards low q values in agreement with the observational measurements in the Sco OB2 association (Shatsky & Tokovinin 2002). For each of the primary and secondary stars that fulfill $M_1 \geq 15M_\odot$ or $M_2 \geq 15M_\odot$, their Hydrogen+Helium burning lifetime is compared to the age of its cluster (τ_{cl}). If the primary star is alive ($\tau_{M1} \geq \tau_{cl}$), the system is included in the statistics with the system mass M_* being substituted by M_1 . Whenever $\tau_{M1} < \tau_{cl}$, the star is considered to have exploded as a supernova. If the secondary star is an O star and it is still alive ($\tau_{M2} \geq \tau_{cl}$), M_2 is used as the system mass. If both stars have already exploded as supernovae or if both are less massive than $15 M_\odot$, the system is removed from the statistics.

Fig. 5 displays two examples of the ICLMF (magenta line), of the corresponding present day cluster mass functions (CLMF) after correcting for binarity and stellar evolution (black line), and of the mass functions of clusters that contain single O-star systems (CLMF-O, triple dot-dash orange line). The left panel corresponds to a case in which the set of three parameters that describe the IMF of each cluster are each randomly drawn from a GPD- σ_{obs} probability distribution function whereas the right panel displays a case in which the set of three parameters that describe the IMF is similar to the values of the parameters for the Galactic field mass function (i.e., δF -GF). In both realizations, the other parameters are set to $\beta = 2$, $SFR = 1 M_\odot$, and $M_{cl,min} = 50 M_\odot$. In both cases, almost all single O stars reside in clusters whose masses are $\leq 400 - 500 M_\odot$. A noticeable difference between the two cases in Fig. 5 is that in the case where the set of the three parameters of the IMF (γ, Γ, M_{ch}) are randomly drawn for each cluster from GPD- σ_{obs} distribution functions, there is a slowly decaying fraction of the clusters that harbor single O stars (i.e., ratio of CLMF-O to CLMF) in contrast to the case where the three parameters of the IMF assigned to the clusters are identical (i.e., δF -GF). This is due to the fact that when the IMF parameters are sampled from broad distribution functions, a significant fraction of the clusters will be assigned steep slopes in the intermediate- to high stellar mass range. Clusters with a steep slope in the intermediate- to high stellar mass range are more likely to harbor single O stars. This is in contrast to the case with an identical Galactic field-like IMF assigned to all clusters (i.e., δF -GF) and where the fraction of clusters that harbor single O stars drops quickly as a function of cluster mass, at high cluster masses (Fig. 5, right panel).

4.4 Correcting for the effects of cluster incompleteness

Before we can compare the models to the observations, it is necessary that each cluster mass function, after the effects of the binary population and stellar evolution are taken into account is also corrected for effects of sample incompleteness. The MWSC sample is affected by incompleteness issues arising from the non-detection of clusters located at large distances from the Sun as well as the non-detection of faint nearby clusters. The completeness correction is calculated for each realization of the cluster mass function with respect to the sample of young clusters in the MWSC survey. In this work, the approach we use to account for the

effect of cluster incompleteness is based on the populations of low mass B stars in the clusters (i.e., stars with masses between $2M_\odot \leq M_* \leq 10M_\odot$) whose total number in a cluster is $N_{*,2-10}$. For each realization of the ICLMF, after the corrections for the effects of the binary population and stellar evolution have been taken into account, we compute the distribution of low mass B stars $\phi(N_{*,2-10})$. Fig. 6 (top panel) displays an example of the distribution of ϕ for one of the ICLMF realizations (full black line) and for the young clusters in the MWSC catalog (purple dashed line) plotted versus $\log(N_{*,2-10} + 1)$. The unnormalized ratio of these two distributions ($R_{2-10} = \phi_{obs}/\phi_{model}$) is plotted in Fig. 6 (middle panel). All functions that we have computed for the different synthetic cluster mass functions display a flattening for $N_{*,2-10} \geq 25$ ($\log(N_{*,2-10}) \geq 1.4$) as can be observed in the example in Fig. 6. Thus, we normalize the function to its value at $\log(N_{*,2-10}) = 1.4$. The normalized R_{2-10} function constitutes the completeness function, f_{comp} . We assume a completeness probability of $f_{comp} = 1$ for any cluster with $\log(N_{*,2-10}) \geq 1.4$. We fit the part of the completeness function for $\log(N_{*,2-10}) < 1.4$ with a power-law function (triple dot-dash line, Fig. 6, lower panel). A cluster is admitted for the comparison with the observational data if its completeness probability f_{comp} is larger than a uniform random number drawn between 0 and 1. For the families of ICLMFs generated in this work, typically only about half of the clusters in the ICLMF pass the filter of the completeness function and are used in the comparison with the observational data.

5 COMPARISON OF MODELS TO OBSERVATIONS

5.1 Models based on stochastic star formation

In this family of models, stellar masses in each cluster are randomly sampled in the mass range $[0.02, \min(M_{cl}, 150)]M_\odot$ for the set of parameters (γ, Γ, M_{ch}) that are assigned to the cluster. When comparing the fractions of single and lonely O stars ($f_{single,O}$ and $f_{lonely,O}$) between the observations and the models of synthetic clusters, we have two main options: we compare the observational values of $f_{single,O}$ and $f_{lonely,O}$ with the same quantities derived for the entire sample of clusters in a given initial cluster mass function that pass the filter of the completeness function (or to an average value of these quantities for a number of realizations of the ICLMF; i.e., "all clusters" approach). Under this approach, the assumption is that the sample of $N_{MWSC,cl} = 102$ clusters in the MWSC that are used to determine the observational values of $f_{single,O}$ and $f_{lonely,O}$ represents an unbiased sample of the Galactic population of the Milky Way stellar clusters. A more accurate approach is achieved by comparing the observational values of $f_{single,O}$ and $f_{lonely,O}$ with the same quantities calculated from subsamples of synthetic clusters of size $N_{MWSC,cl} = 102$ (i.e., subsamples approach). The subsamples are randomly drawn from the (much) larger samples of synthetic clusters that pass the filter of the completeness function in each realization of the ICLMF. For each realization of the ICLMF, we generate 10000 subsamples of size $N_{MWSC,cl}$ and for each subsample, we calculate The values of $f_{single,O}$ and $f_{lonely,O}$.

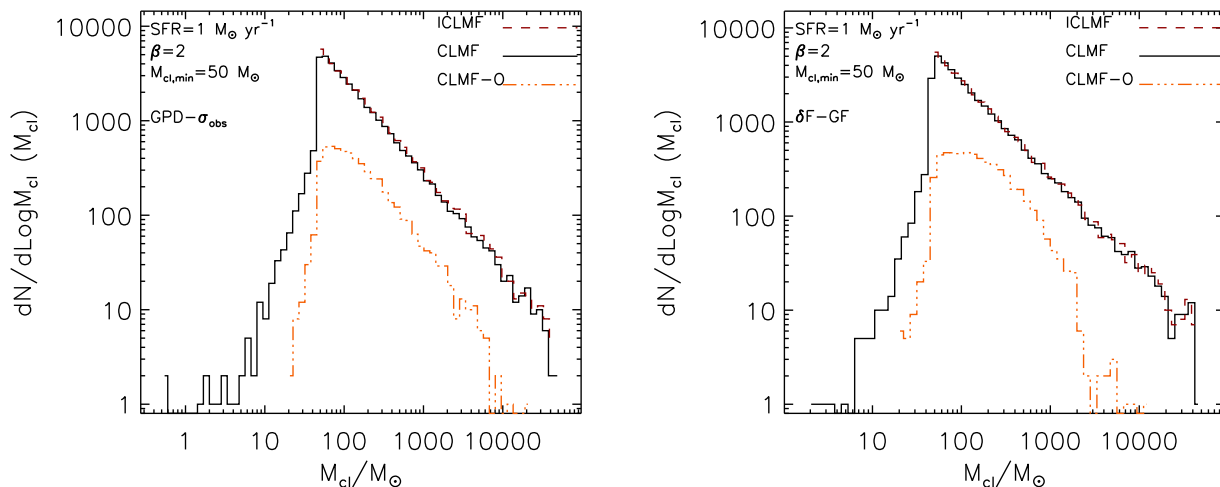


Figure 5. the initial, present-day, and single O-star cluster mass functions in two realizations of the ICLMF. The left panel displays a case in which the set of three parameters that describe the IMF of each cluster are each randomly drawn from a GPD- σ_{obs} probability distribution function whereas the right panel displays a case in which the set of three parameters that describe the IMF is similar to the values of the parameters for the Galactic field mass function. All other parameters are set to $M_{cl,min} = 50 M_{\odot}$, $M_{*,min} = 0.02 M_{\odot}$, $M_{*,max} = 150 M_{\odot}$, and $\beta = 2$. The figure displays the initial cluster mass function (ICLMF) and the present-day cluster mass function (CLMF). The CLMF is the conversion of the ICLMF after each individual cluster has been assigned an age, and has been corrected for the effects of the stellar binary fraction and stellar evolution. The number distribution of clusters that contain single O stars (with $M_* \geq 15 M_{\odot}$ (CLMF-O), peaks at a few tens of stellar masses and most of the clusters in the CLMF-O have masses $\lesssim 400 M_{\odot}$.

Fig. 7 displays the distributions of $f_{single,O}$ and $f_{lonely,O}$ for one realization of ICLMF. The example displayed in Fig. 7 corresponds to a realization of the ICLMF with the parameters $SFR = 1 M_{\odot} \text{ yr}^{-1}$, $\beta = 2$, and $M_{cl,min} = 50 M_{\odot}$, and where the set of the three parameters that describe the IMF of each cluster are each randomly drawn from a GPD- σ_{obs} probability distribution function.

In Fig. 8 (panel A), we compare the values of $f_{single,O}$ and $f_{lonely,O}$ in the MWSC to those derived from the models of synthetic clusters generated with the various prescriptions for the distributions of the three IMF parameters. All other parameters of the models have similar values ($\beta = 2$, $M_{cl,min} = 50 M_{\odot}$). Each estimate of $f_{single,O}$ and $f_{lonely,O}$ in the “all sample” approach (orange points in Fig. 8) is a mean value over 27 realizations based on three different random seeds for filling the ICLMF and the corresponding IMFs of the clusters, three permutations of the value of the Galactic SFR, and three permutations for the randomly assigned ages of the clusters. The associated error bars are the dispersion measured from these 27 realizations. The purple points and associated error bars are the grand mean and grand mean absolute deviation from the 27 ICLMF realizations and where the mean and mean absolute deviation for each realization are calculated from the 10000 drawings of subsamples of clusters each of size $N_{MWSC,cl} = 102$. The use of the mean absolute deviation to estimate the uncertainty in this case is more judicious than the standard deviation as it is less sensitive to extreme outliers in the randomly drawn subsamples.

As can be observed in Fig. 8 (panel A), an agreement between the observations and the simulated clusters can only be achieved when the distributions of the IMF parameters are Gaussian function that have significant intrinsic widths

that are close to $\approx (\sigma_{\Gamma_{obs}}, \sigma_{\gamma_{obs}}, \sigma_{M_{ch,obs}})$. The equally good agreement between the FPD model and the observations shows that the results are not extremely sensitive to the exact shape of the distribution functions of the parameters. Future larger data sets of Galactic clusters will help better constrain the exact shape of the distribution functions of the parameters. Fig. 8 (panel A) also shows that no agreement is found between the observations and the models with narrow distributions of the IMF parameters and in particular when the distributions are delta functions located at either the values of the parameters for the Galactic field or at the mean values derived for the sample of young clusters by Dib (2014a).

We also explore the effects of varying the exponent of the ICLMF and of the lower cluster mass cutoff for fixed values of the width of the Gaussian distributions (fixed at $\sigma_{\gamma_{obs}}$, $\sigma_{\Gamma_{obs}}$, and $\sigma_{M_{ch,obs}}$, for the distributions of γ , Γ , and M_{ch} , respectively). We show in Fig. 8 (panel B) the predicted single and lonely O star fractions for three values of $\beta = 1.8, 2$, and 2.2 . A change in the values of β strongly affects the relative fraction of low mass- to massive clusters, which translates into significant variations in the fraction of single and lonely O-stars. Steeper/shallower values of β result in a larger/smaller fraction of low mass clusters which are more/less likely to harbor single and lonely O stars. The comparisons in Fig. 8 (panel B) constrain β to be very close to 2. The effect of changing the lower mass cutoff of the ICLMF ($M_{cl,min}$) is displayed in Fig. 8 (panel C). The comparison when $M_{cl,min}$ is 10, 20 and $50 M_{\odot}$ shows that the fractions of single and lonely O stars are not extremely sensitive to the value of the lower mass cutoff. This implies that the ICLMF may well extend to masses close to $10 M_{\odot}$.

Stars in clusters interact dynamically, and three-body

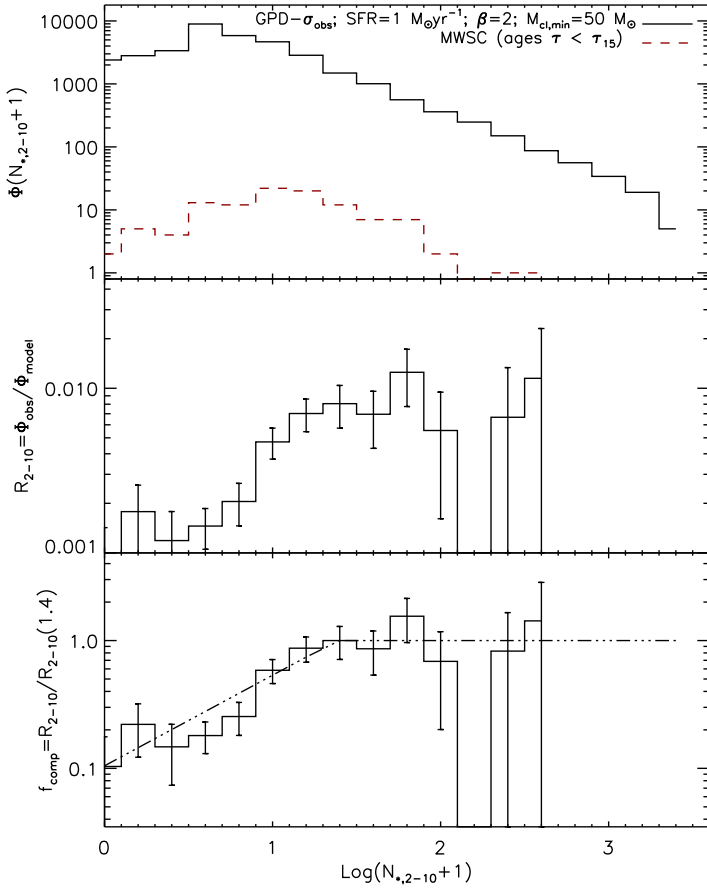


Figure 6. The completeness correction is based on the clusters low mass B star systems population (star-systems with masses between $2M_{\odot} \leq M_* \leq 10M_{\odot}$). The top panel displays the distribution of the total number of low mass B stars/systems ($N_{*,2-10}$) for one realization of the ICLMF (black full line) and for the ensemble of young clusters in the MWSC catalog (dashed purple line). The middle panel displays the ratio (R_{2-10}) of $N_{*,2-10}$ in the observations to the model. The lower panel displays the ratio of R_{2-10} normalized to its value at $\log(N_{*,2-10}) = 1.4$. The quantity $f_{comp} = R_{2-10}/R_{2-10}(1.4)$ defines the completeness. The completeness function is approximated by a value of unity for $\log(N_{*,2-10}) \geq 1.4$ and by a linear fit for $\log(N_{*,2-10}) < 1.4$. The fit to the completeness function is shown for this example with the triple dot-dash line.

interactions can lead to the ejection of stars or binary systems. The fraction of O stars that are ejected can vary widely from cluster to cluster, and can depend on the mass of the cluster, its half mass radius, the degree of primordial mass segregation of stars in the cluster, the binary fraction, mass ratios in massive binaries, and the period distributions of massive systems. For the most realistic estimates of these parameters, the fraction of ejected O stars has been estimated to be negligible for clusters whose masses are $\leq 400 - 500 M_{\odot}$. It increases up to $\approx 25\%$ for cluster masses of $\approx 3000 M_{\odot}$ and declines to $5 - 10\%$ for higher cluster masses (Oh et al. 2015). Note that these fractions were evaluated for clusters that obey an $M_{cl} - M_{*,max}$ relation and all possess the same underlying Galactic field-like IMF (i.e., the Kroupa IMF). As such, these estimates may not reflect exactly the expected fractions of ejected O stars for each family of our synthetic clusters. However, the basic result, that dy-

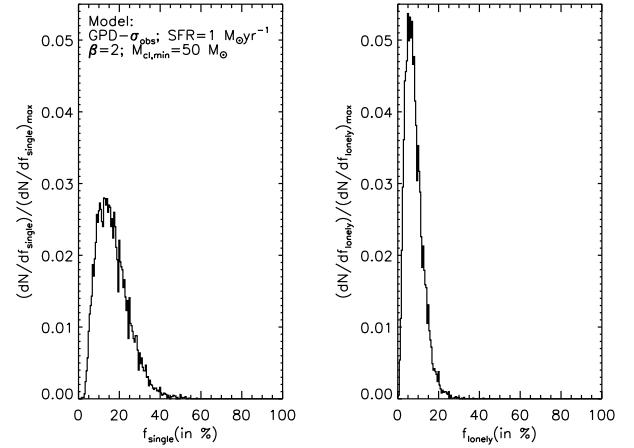


Figure 7. The distributions of $f_{single,O}$ and $f_{lonely,O}$ are generated using measurements of these two quantities over 10000 randomly chosen ensemble of clusters, each of size equal to the size of young clusters in the MWSC catalog ($N_{MWSC,cl} = 102$). Each subsample of clusters of size $N_{MWSC,cl}$ is drawn from the larger sample of clusters that pass the filter of the completeness function in a given realization of the ICLMF. The example displayed here corresponds to one realization of the ICLMF with the parameters $SFR = 1 M_{\odot} \text{ yr}^{-1}$, $\beta = 2$, $M_{cl,min} = 50 M_{\odot}$, and where the set of three parameters that describe the IMF of each cluster are each randomly drawn from a GPD- σ_{obs} probability distribution function.

namical ejection of O stars from clusters less massive than $\approx 400 - 500 M_{\odot}$ is insignificant, should not depend on these details. Since most clusters that harbor single O stars in our models have masses $< 400 - 500 M_{\odot}$, the ejection of massive stars from the clusters is not expected to significantly affect the value of $f_{single,O}$. If we account for the fraction of ejected O stars, The quantity $f_{single,O}$ can be approximated by $\approx N_{single,O} / (N_{single,O} + f_O N_{non-single,O})$, where $N_{non-single,O}$ is the number of O star that are not single, and f_O is the fraction of ejected O stars as a function of the cluster mass. Using the values of $N_{single,O}$ and $N_{non-single,O}$ and adapted values of f_O as a function of cluster mass for the different families of models yields small increases in $f_{single,O}$ of $\approx 10 - 12\%$ for GPD- σ_{obs} type models and $\approx 18 - 22\%$ for δF -GF type models. Applying this correction to account for the fraction of dynamically ejected O stars increases the disagreement between the δF -GF type models and the observations while at the same time, it does not substantially affect the relative good agreement between the GPD- σ_{obs} models and the observations.

5.2 Models with an imposed $M_{cl} - M_{*,max}$ relation

Our modeling allows us to test the consequences of constraining the maximum stellar mass in clusters. Weidner & Kroupa (2004) argued that a deterministic relation exists between the mass of the most massive star in a cluster and the mass of the cluster. The existence of a cluster-mass-dependent truncation of the IMF is highly debated and has important consequences for cluster and galaxy properties and evolution. A $M_{cl} - M_{*,max}$ relation results in a steeper galaxy wide IMF for lower mass galaxies at a fixed SFR and

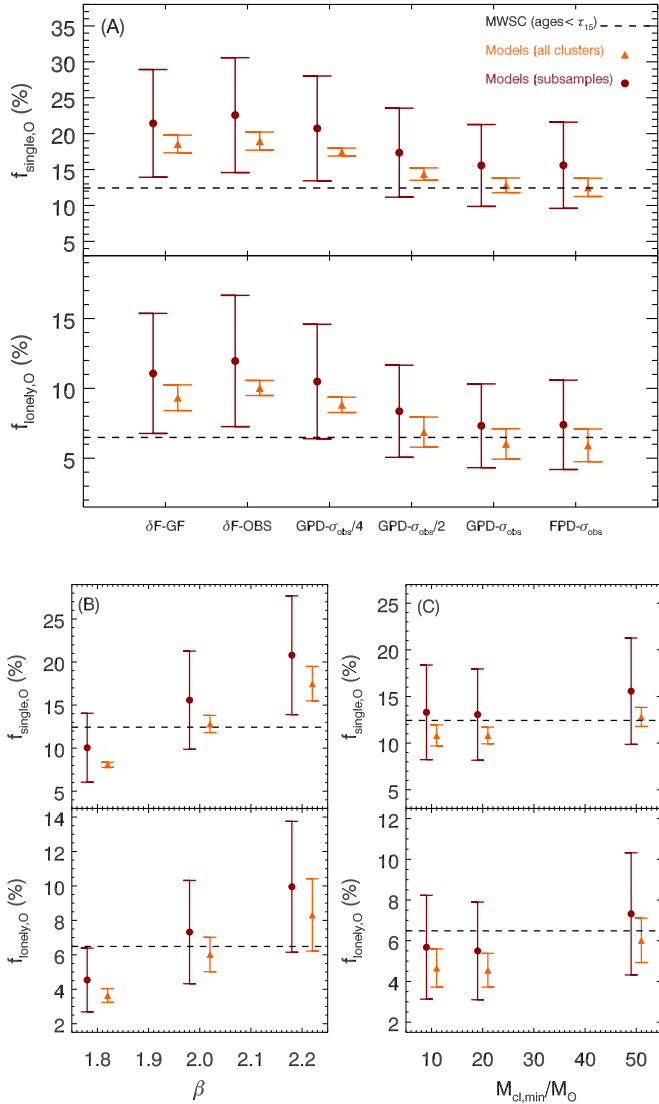


Figure 8. The top panel (A) in the figure compares the fractions of single and lonely O-star systems (defined as $M_* \geq 15 M_{\odot}$) calculated from the samples of clusters from the MWSC survey (dashed lines) with those measured for the different models of synthetic clusters (purple circles and orange triangles). The other parameters of the models are set at their fiducial values of $M_{cl,min} = 50 M_{\odot}$, $M_{*,min}=0.02 M_{\odot}$, $M_{*,max} = 150 M_{\odot}$, and $\beta = 2$. The orange points and error bars are the mean and standard deviation of $f_{single,O}$ and $f_{lonely,O}$ calculated using all clusters that pass the filter of the completeness function in 27 realizations of the initial cluster mass function (ICLMF). The 27 realizations include variations of the Galactic star formation rates, the randomly drawn ages of the clusters, and seed numbers used to randomly sample the ICLMF and the stellar masses within each cluster. The purple points and error bars are the grand mean and grand mean absolute deviation from the 27 ICLMF realizations and where the mean and mean absolute deviation for each realization are calculated from 10000 drawings of subsamples of clusters each of size $N_{MWSC,cl} = 102$. Each subsample of $N_{MWSC,cl}$ clusters is randomly drawn from the ensemble of clusters that pass the filter of the completeness function in each realization of the ICLMF. The lower left panel (B) and lower right panel (C) display the effect of changing the exponent of the ICLMF (β) and the minimum cluster mass ($M_{cl,min}$), respectively. For clarity, the orange triangles and purple circles have been shifted horizontally by $[0.2, -0.2]$, and by $[1, -1]$ in panels (B) and (C), respectively.

to a downturn in the ratio of the H α emission to the Far Ultraviolet emission (FUV) at low galactic FUV luminosities. A number of observational studies found that a cluster-mass-dependent truncation of the IMF leads to an underprediction of the observed H α luminosities at low FUV luminosity (Fumagalli et al. 2011; Weisz et al. 2012). Other studies on the scale of resolved star forming regions using the H α /FUV ratios or the correlation between H α and bolometric luminosities found results that do not seem to lend support to the existence of an $M_{cl} - M_{*,max}$ relation (Hermanowicz et al. 2013).

Following the same procedure described above, we generate additional models in which the masses of stars (i.e., star-systems) in the clusters are randomly sampled in the range $M_{*,min} = 0.02 M_{\odot}$ and an $M_{*,max}$ that is imposed by the latest version of the $M_{cl} - M_{*,max}$ relation (Weidner et al. 2013). The $M_{cl} - M_{*,max}$ relation is given by $\log_{10}(M_{*,max}/M_{\odot}) = -0.66 + 1.08 \times [\log_{10}(M_{cl}/M_{\odot})] - 0.15 \times [\log_{10}(M_{cl}/M_{\odot})]^2 + 0.0084 \times [\log_{10}(M_{cl}/M_{\odot})]^3$ and is assumed to be valid for cluster masses $M_{cl} \leq 2.5 \times 10^5 M_{\odot}$ which is the case of the clusters considered in this work. All other parameters are kept at their fiducial values. We measure $f_{single,O}$ and $f_{lonely,O}$ in this additional set of models. The results displayed in Fig. 9 (Panel C) show that these models do not satisfactorily reproduce the observations. While the comparison using $f_{single,O}$ is inconclusive, imposing a $M_{cl} - M_{*,max}$ relation leads to an underestimate of $f_{lonely,O}$ by a factor of ≈ 3 for all models with respect to the observational value. This conclusion is not sensitive to the choice of β and $M_{cl,min}$ (Fig. 9, panels E and F, respectively).

5.3 Additional predictions

The primary goal of this work is to provide a method that allows us to assess the universality of the IMF for the population of Galactic stellar clusters across the entire stellar mass range and that is based solely on the clusters stellar populations of massive O stars (for discriminating between IMF models) and B stars (for accounting for the completeness effects). The method does not rely on the knowledge of the exact total number of stars (N_*) in the clusters, nor does it rely on the knowledge of the masses of the low mass stars (i.e., masses $M_* < 2 M_{\odot}$). Nevertheless, with this approach, it is possible to make a number of additional predictions for the models with the different families of the IMF parameters distribution functions. These predictions can be contrasted with additional observational constraints, when available. Fig. 10 displays a 2D histogram of the relationship between the numbers of stars found in clusters (N_*) and the maximum stellar mass in the clusters ($M_{max,*}$) for two realizations of the ICLMF. One of these realizations of the ICLMF uses $GPD-\sigma_{obs}$ distributions functions of the IMF parameters (left panel) and the other $\delta F-GF$ distributions of IMF parameters (right panel). The results displayed in Fig. 10 suggest the existence of a different $N_* - M_{*,max}$ relation between these models. The observational data overlaid to the models in Fig. 10 comes from a compilation of young clusters by (Maschberger & Clarke 2008). We only include clusters with an observational value of $N_* \geq 25$. While the number of observed clusters in this compilation is relatively small compared to the number of clusters in each of

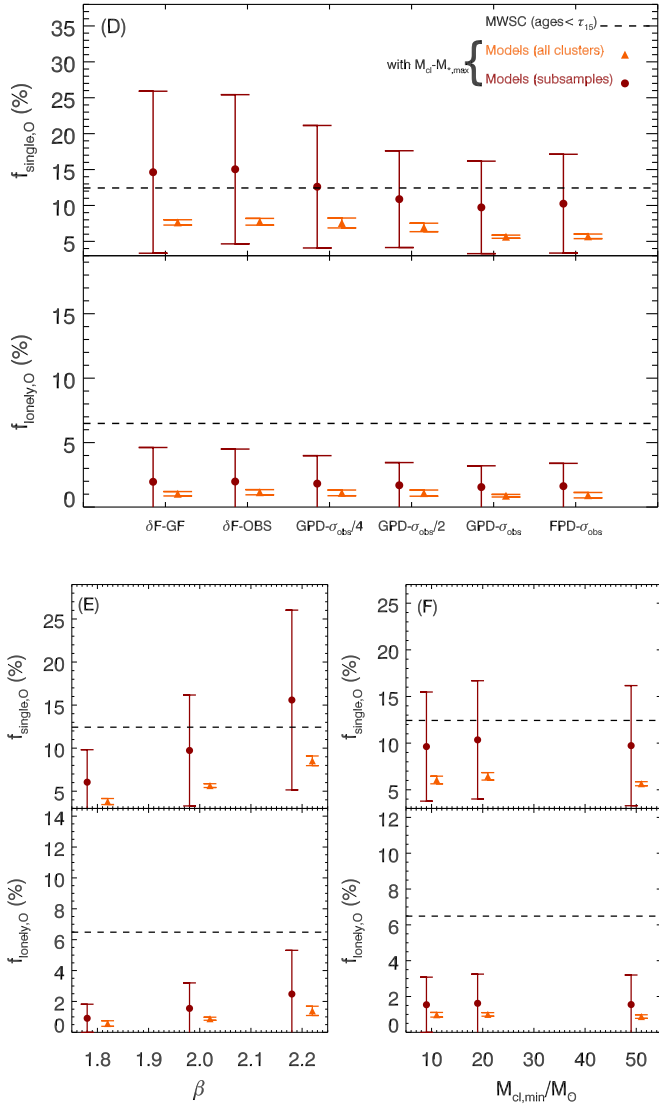


Figure 9. Effects of the cluster mass (M_{cl})-maximum stellar mass ($M_{*,\text{max}}$) relation on the fraction of single and lonely O stars. This figure is similar to Fig. 8 with the exception that there is an imposed $M_{\text{cl}} - M_{*,\text{max}}$ relation which determines the maximum mass a star can have when sampling stellar masses in a cluster of mass M_{cl} (see text for more details). For clarity, the orange triangles and purple circles have been shifted horizontally by $[0.2, -0.2]$ and by $[1, -1]$ in panels (E) and (F), respectively

the simulated models, we can tentatively argue that the observational data points in Fig. 10 lie closer to the peak of the 2D distributions when the IMF parameters are described by the $\text{GPD-}\sigma_{\text{obs}}$ case versus the $\delta F\text{-GF}$ case. Fig. 11 displays the cluster mass (M_{cl}) - Number of O stars more massive than $15 M_{\odot}$ ($N_*(M_*/M_{\odot} > 15)$) relation for the same two realizations with the $\text{GPD-}\sigma_{\text{obs}}$ and the $\delta F\text{-GF}$ distribution functions of the IMF parameters. Here also, noticeable differences can be observed in this scatter relation. In particular, there is a much tighter correlation between M_{cl} and $N_*(M_*/M_{\odot} > 15)$ for the case with a universal IMF ($\delta F\text{-GF}$), particularly at higher cluster masses.

6 COMPARISON TO PREVIOUS WORK

To the best of our knowledge, this paper presents the first attempt to constrain the distribution functions of the set of parameters that describe the shape of the IMF over the entire stellar mass range for a large population of young clusters in the Milky Way. Models of synthetic clusters have been used by other authors in order to infer the fraction of single (or isolated⁶) O stars and compare it to the putative fraction of isolated O star in the Galactic field (e.g., de Wit et al. 2005; Parker & Goodwin 2007; Lamb et al. 2010; Weidner et al. 2013). In all of these models however, zero-age age clusters were always constructed under the assumption of a universal IMF and most of them did not include additional corrections (binarity, stellar evolution, and incompleteness effects). Interestingly, Parker & Goodwin (2007) found values of $f_{\text{single},O}$ and $f_{\text{lonely},O}$ of 16.7% and 9.7% when sampling the IMF in clusters stochastically, for a ICLMF with $\beta = 2$, and using a Kroupa-like constant Galactic field IMF (see Table 1 in their paper). These values are in relative good agreement with the values we find using the $\delta F\text{-GF}$ family of models (Fig. 8), and both are higher than the corresponding values measured from the MWSC. They also found that these fractions are reduced by a factor of $\approx 2 - 3$ when stellar masses are randomly sampled under the constraint of an $M_{\text{cl}} - M_{*,\text{max}}$ relation.

7 DISCUSSION

The debate over the universality or potential variation of the IMF among stellar clusters, as well as the similarity between the IMF in clusters and the Galactic field stellar mass function has been ongoing ever since Salpeter (1955) published his findings. From a theoretical point of view, much of the arguments in favor/disfavor of variations of the IMF originate from the inclusion/absence in the models of the necessary physical processes that can lead to a significant degree of variations. A perfect illustration of this are the contrasting conclusions made by Dib et al (2010) and Hennebelle (2012). Dib et al. (2010) considered the case of accreting protostellar cores in a non-accreting star forming clump whereas Hennebelle (2012) considered the case of non-accreting cores in an accreting clump. Dib et al. (2010) showed that the accretion of gas by protostellar cores can lead to variations in the core mass function (and hence of the IMF) when environmental conditions vary from clump-to-clump Dib et al. (2010) and Dib (2014b) showed that a Taurus-like mass function can be reproduced when protostellar cores continue to accrete over longer timescales (i.e., as a result of being supported by stronger magnetic fields), and this leads to the depletion of the population of low mass cores and shifts the peak of the mass function towards higher masses. In contrast, in the model of Hennebelle (2012), the accretion of gas by the clump from the larger scale environment is only expected to change the thermodynamical properties of the gas out of which newer generations of stars can form in the clump. Hennebelle (2012) finds that the position of the peak

⁶ both de Wit et al. (2007) and Parker & Goodwin (2007) define an O star as a single star in a cluster with $M_* \geq 17.5 M_{\odot}$, and B stars as stars with $10 M_{\odot} \leq M_* \leq 17.5 M_{\odot}$

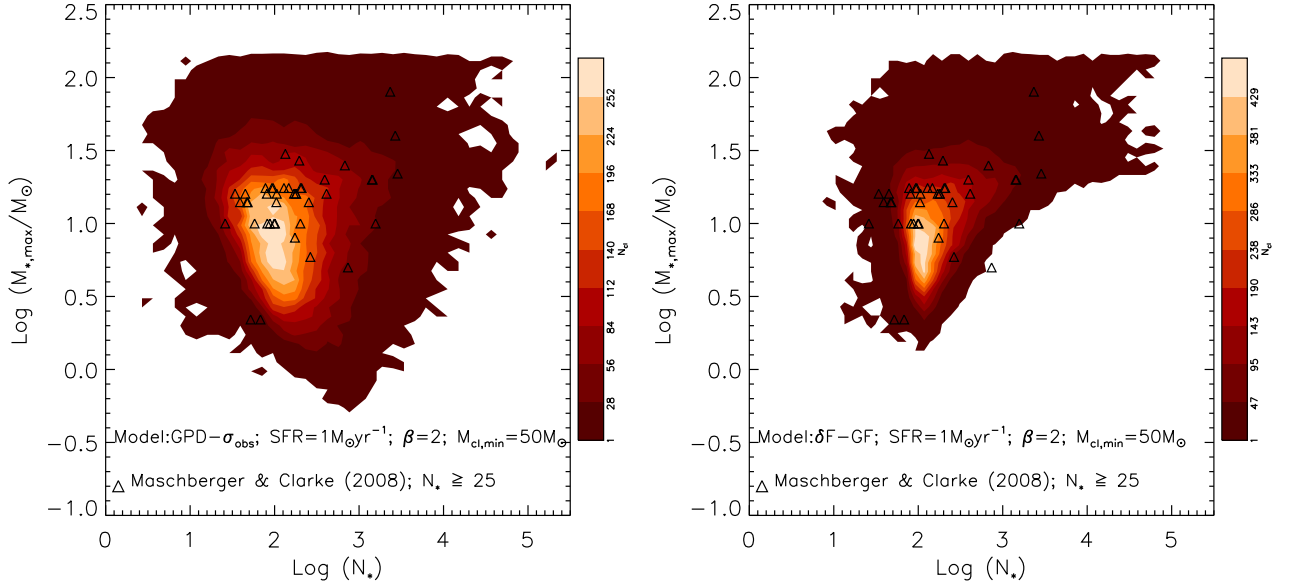


Figure 10. The $N_* - M_{*,\text{max}}$ relation. Comparison of the relationship between the number of stars in the clusters (N_*) and the mass of the most massive star in the clusters ($M_{*,\text{max}}$) in two realizations of the ICLMF. The left panel displays a case in which the set of three parameters that describe the IMF of each cluster are each randomly drawn from a GPD- σ_{obs} probability distribution function whereas the right panel displays a case in which the set of three parameters that describe the IMF is similar to the values of the parameters for the Galactic field mass function. Overlaid are observational data compiled by Maschberger & Clarke (2008).

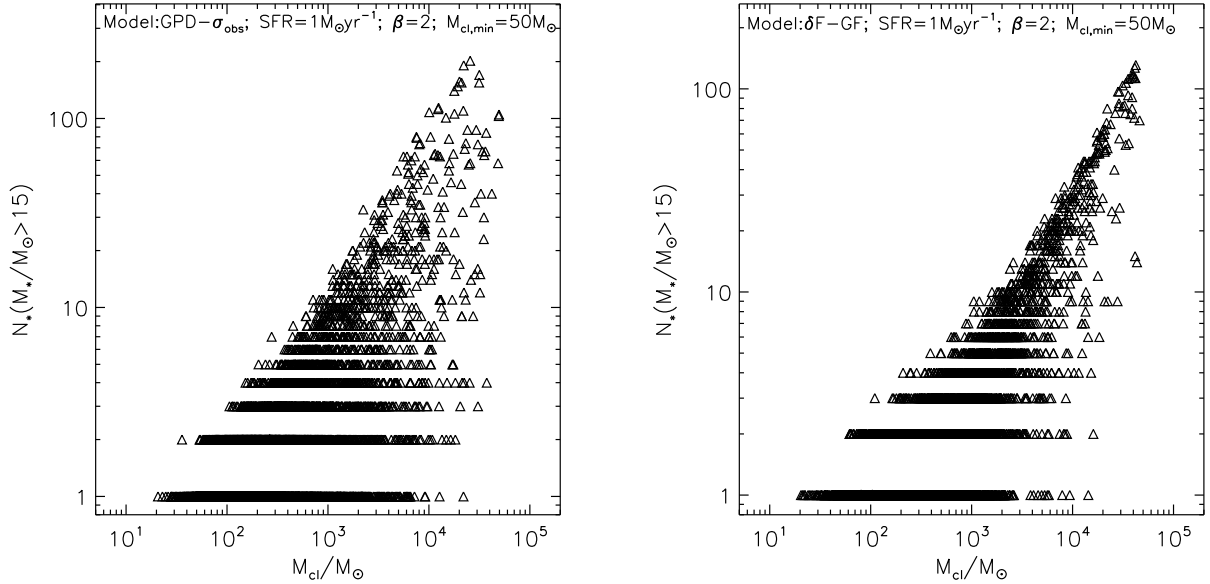


Figure 11. The $N_*(M_*/M_\odot > 15) - M_{\text{cl}}$ relation. Comparison of the relationship between the mass of the cluster (M_{cl}) and the number of stars more massive than $15 M_\odot$ ($N_*(M_*/M_\odot > 15)$) present in each cluster in two realizations of the ICLMF. The left panel displays a case in which the set of three parameters that describe the IMF of each cluster are each randomly drawn from a GPD- σ_{obs} probability distribution function whereas the right panel displays a case in which the set of three parameters that describe the IMF is similar to the values of the parameters for the Galactic field mass function.

of the IMF is not extremely sensitive to the thermodynamical conditions of the star forming gas, as earlier suggested by Elmegreen et al. (2008), and more recently confirmed by Krumholz et al. (2016).

Several observational studies have also reported that the slope of the IMF at the high mass end of starburst clusters such as the Arches cluster, NGC 3603, and the Quintuplet cluster might be shallower than the Salpeter value (e.g., Harayama et al. 2008; Espinoza et al. 2009). Shadmehri (2004) and Dib et al. (2007, 2008) and Dib (2007) proposed that shallower-than Salpeter slopes can result from the efficient coalescence of closely packed protostellar cores in a dense protocluster environment.

8 CONCLUSIONS

In this work, we test the universality of the IMF by comparing the fractions of single (i.e., isolated) and lonely O (single in their clusters and absence of massive B stars) stars in a sample of Galactic clusters and in synthetic cluster models constructed with various prior functions from which the parameters of the individual IMFs are randomly drawn. Using a Monte Carlo approach, the masses of stellar clusters are randomly sampled from an initial cluster mass function that is described by a power-law distribution. The initial stellar mass function of stars within each cluster is randomly sampled using the tapered power-law mass function. In order to make synthetic clusters resemble the observations, each cluster is assigned an age which is randomly drawn from a flat distribution function similar to the observations, and are corrected for the effects of binary population and stellar evolution. Different models are constructed in which the set of three parameters that describe the TPL-IMF (i.e., the slope at the high mass end, the slope at the low mass, and the characteristic mass) assigned to each cluster are randomly sampled from parent distributions of varying widths, going for delta functions corresponding to the case of universal IMF to broad distributions of the IMF parameters. After correcting for the effect of incompleteness, we compare the fractions of single and lonely O stars in these various models of simulated clusters with the fractions of single and lonely O stars measured for the population of young stellar clusters in the Milky Way.

Our work provides strong evidence that the fraction of single and lonely O stars in young stellar clusters implies a non-universal IMF. Broad distributions of the parameters that describe the shape of the IMF are required in order to reproduce the observed fractions of single and lonely O stars in the Milky Way stellar clusters. These broad distributions are compatible with the scatter between the IMF parameters of a more limited number of clusters found recently by Dib (2014a). On the other hand, we show that narrow distributions of the IMF parameters that are associated with the concept of a universal IMF are not favored by our results. The method also allows us to put constraints on the shape of the initial cluster mass function. We find that the observational data is better matched with an exponent of the power-law initial cluster mass function of -2 . Furthermore, our results suggest that star formation in clusters is stochastic and do not lend support to the existence of a deterministic cluster mass-maximum stellar

mass relation. When the IMF is described by the tapered power-law, we propose that the parameters of the probabilistic IMF (γ, Γ, M_{ch}) be described by Gaussian probability distributions with the following standard deviations $\sigma_{\gamma_{obs}} = 0.25$, $\sigma_{\Gamma_{obs}} = 0.6$, $\sigma_{M_{ch,obs}} = 0.27 M_{\odot}$, and centered around $\gamma_{obs} = 0.91$, $\Gamma_{obs} = 1.37$, and $M_{ch,obs} = 0.41 M_{\odot}$, respectively.

The broad distributions of the IMF parameters inferred in this work very likely reflect the existence of equally broad distributions for the initial conditions under which these clusters have formed in Galactic proto-cluster clumps (e.g., Svoboda et al. 2016). As such, they offer an important motivation to explore physical mechanisms that can cause the IMF to vary from one star-forming region to another (e.g., different level of accretion rates onto protostars, mergers of protostars, and the effects of feedback and triggering). The implications of our results are manifold. For example, the probabilistic IMF proposed in this work, in lieu of a fixed IMF, is expected to influence the modeling of star formation and stellar feedback in sub-grid models that are employed in cosmological simulations. Broad distributions of the IMF parameters imply less feedback and chemical enrichment in star forming regions with a steep slope of the IMF in the high mass regime versus more feedback and chemical enrichment in star forming regions with a shallow slope in this mass regime.

ACKNOWLEDGMENTS

S. D. is supported by a Marie-Curie Intra European Fellowship under the European Community's Seventh Framework Program FP7/2007-2013 grant agreement no 627008. This work was supported by a research grant (VKR023406) from the Villum Foundation. S. S. was supported by Sonderforschungsbereich SFB 881 The Milky Way System (sub-project B5) of the German Research Foundation (DFG). S. H. acknowledges financial support from DFG programme HO 5475/2-1. This research has made use of NASA's Astrophysics Data System Bibliographic Services.

REFERENCES

- Alves de Oliveira, C., Moraux, E., Bouvier, J., et al. 2013, *A&A*, 549, 123
- Ascenso, J., Alves, J., Vicente, S., Lago, M. T. V. T. 2007, *A&A*, 476, 199
- Basu, S., Gil, M., Auddy, S. 2015, *MNRAS*, 449, 2413
- Bochanski, J. J., Hawley, S. L., Covey, K. R., West, A. A., Reid, I. N., Golimowski, D. A.; Ivezić, Z. 2010, *AJ*, 139, 2679
- Boissier, S., Prantzos, N. 1999, *MNRAS*, 307, 857
- Bouvier J., Kendall, T., Meeus, G. et al. 2008, *A&A*, 481, 661
- Carpenter, J. M. 2000, *MNRAS*, 120, 3139
- Chabrier, G. 2003, *PASP*, 115, 763
- Chabrier, G. 2005, in *Astrophysics and Space Science Library*, Vol. 327, *The Initial Mass Function 50 Years Later*, ed. E. Corbelli, F. Palla, & H. Zinnecker, 41
- Chandar, R., Fall, S. M., Whitmore, B. C. 2010, *ApJ*, 711, 1263
- Chini, R., Hoffmeister, V. H., Nasser, A., Stahl, O., Zinnecker, H. 2012, *MNRAS*, 424, 1925
- Clark, J. S., Negueruela, I., Davies, B., Larionov, V. M., Richie, B. W. et al. 2009, *A&A*, 498, 109
- de Grijs, R., Anders, P. 2006, *MNRAS*, 366, 295

- Delgado, A. J., Alfaro, E., J., Yun, J. L. 2011, *A&A*, 531, 141
- De Marchi, G., Paresce, F., Portegies Zwart, S. 2010., *ApJ*, 718, 23
- de Wit, W. J., Testi, L., Palla, F., Zinnecker, H. 2005, *A&A*, 437, 247
- Dib, S., Bell, E., Burkert, A. 2016, *ApJ*, 638, 797
- Dib, S. 2007, *JKAS*, 40, 157
- Dib, S., Kim, J., Shadmehri, M. 2007, *MNRAS*, 381, L40
- Dib, S., Shadmehri, M., Gopinathan, M., Kim, J., Henning, Th. 2008, in *Massive Star Formation: Observations confront Theory*, ASP Conf. Series, Ed. H. Beuther, H. Linz, T. Henning, 387, 282
- Dib, S., Shadmehri, M., Padoan, P., Maheswar, G., Ojha, D. K., Khajenabi, F. 2010b, *MNRAS*, 405, 401
- Dib, S., Piau, L., Mohanty, S., Braine, J. 2011, *MNRAS*, 415, 3439
- Dib, S. 2011, in *Stellar Clusters & Associations: A RIA Workshop on GAIA*, Eds. E. J. Alvaro Navarro, A. T. Gallego Calvente, M. R. Zapatero Osorio, 30
- Dib, S., Gutkin, J., Brandner, W., Basu, S. 2013, *MNRAS*, 436, 3727
- Dib, S. 2014a, *MNRAS*, 444, 1957
- Dib, S. 2014b, in *The Labyrinth of Star Formation*, ed. D. Stamatellos, S. Goodwin, & D. Ward-Thompson (Springer)
- Ekström, S., Georgy, C., Eggenberger, P., Meynet, G., Mowlavi, N. et al. 2012, *A&A*, 537, 136
- Elmegreen, B. G., Efremov, Y. N. 1997, *ApJ*, 480, 235
- Elmegreen, B. G. 2004, *MNRAS*, 354, 367
- Elmegreen, B. G., Klessen, R. S., Wilson, C. D. 2008, *ApJ*, 681, 365
- Espinoza, P., Selman, F. J., Melnick, J. 2009, *A&A*, 501, 563
- Fall, S. M., Chandar, R. 2012, *ApJ*, 752, 96
- Figer, D. F., McLean, I. S., Morris, M. 1999, *ApJ*, 514, 202
- Fumagalli, D., da Silva, R. K., Krumholz, M. R. 2011, 741, 26
- Gennaro, M., Brandner, W., Stolte, A., Henning, Th. 2011, *MNRAS*, 412, 2469
- Girardi, L., Bertelli, A., Bressan, C., Chiosi, C., Groenewegen, M. A. T. et al. 2002, *A&A*, 391, 195
- Haas, M. R., Anders, P. 2010, *A&A*, 512, 79
- Harayama, Y., Eisenhauer, F., Martins, F. 2008, *ApJ*, 675, 1319
- Hermanowicz, M. T., Kennicutt, R. C., Aldridge, J. J. 2013, 432, 3097
- Hunter, D. A., Elmegreen, B. G., Dupuy, T. J., Mortonson, M. 2003, *AJ*, 126, 1836
- Kharchenko, N. V., Piskunov, A. E., Schilbach, E., Röser, S., Scholz, R.-D. 2012, *A&A*, 543, 156
- Kharchenko, N. V., Piskunov, A. E., Schilbach, E., Röser, S., Scholz, R.-D. 2013, *A&A*, 558, 53
- Kobulnicky, H. A., Kimiki, D. C., Lundquist, M. J., Burke, J., Chapman et al. 2014, *ApJS*, 213, 34
- Kroupa, P., Tout, C. A., Gilmore, G. 1993, *MNRAS*, 262, 545
- Kroupa, P. 2001, *MNRAS*, 322, 231
- Lada, C. J., Lada, E. A. 2003, *ARA&A*, 41, 57
- Lamb, J. B., Oey, M. S., Werk, J. K., Ingleby, L. D. 2010, *ApJ*, 725, 1886
- Larsen, S. S. 2009, *A&A*, 494, 539
- Lim, B., Sung, H., Hur, H., Park, B.-G., 2015, in the proceedings of IAU 316, Eds. C. Charbonnel, A. Nota, arXiv: 1511.01118
- Liu, Q., de Grijs, R., Deng, L. C., Hu, Y., Baraffe, I., Beaulieu, S. F. 2009, *MNRAS*, 396, 1665
- Liu, W. M., Meyer, M. R., Cotera, A. S., Young, E. T. 2003, *AJ*, 126, 1665
- Lodieu, N., Dobbie, P. D., Hambly, N. C. 2011, *A&A*, 527, 24
- Luhman, K. L. 2004, *ApJ*, 617, 1216
- Luhman, K. L. 2007, *ApJ*, 173, 104
- Mallick, K. K., Ojha, D. K., Tamura, M., Pandey, A. K., Dib, S. et al. 2014, *MNRAS*, 443, 3218
- Marigo, P., Girardi, L., Bressan, A., et al. 2008, *A&A*, 482, 883
- Martizzi, D., Fielding, D., Faucher-Giguère, C.-A., Quataert, E. 2016, *MNRAS*, 561, in press
- Maschberger, T., Clarke, C. J. 2008, *MNRAS*, 391, 711
- Maschberger, T. 2013, *MNRAS*, 429, 1725
- Massey, P. 1998, in the *Stellar Initial Mass Function*, Eds. G. Gilmore, & D. Howell (San Francisco: ASP), vol 142 of ASP Conf. Ser. 17
- Massey, P. 2011, in the proceedings of UP2010: Have Observations Revealed a Variable Upper End of the Initial Mass Function? M. Treyer, T.K. Wyder, J.D. Neill et al. (eds.) (San Francisco: ASP), ASP Conf. Ser 440, p. 29
- Miller, G. E., Scalo, J. M. 1979, *ApJS*, 41, 513
- Morales, E., Kroupa, P., Bouvier, J. 2004, *A&A*, 426, 75
- Oh, S., Kroupa, P., Pflamm-altenburg, J. 2015, *ApJ*, 805, 92
- Ojha, D. K., Kumar, M. S. N., Davis, C. J., Grave, J. M. C. 2010, *MNRAS*, 407, 1807
- Parker, R. J., Goodwin, S. P. 2007, *MNRAS*, 380, 1271
- Parravano, A., McKee, C. F., Hollenbach, D. J. 2011, *ApJ*, 726, 27
- Preibisch, T., Brown, A. G. A., Bridges, T., Gunether, E., Zinnecker, H. 2002, *AJ*, 124, 404
- Robitaille, T. P., Whitney, B. A. 2010, *ApJ*, 710, 11
- Rybicki, J., Just, A. 2015, *MNRAS*, 447, 3880
- Salpeter, E. E. 1955, *ApJ*, 121, 161
- Scalo, J. M. 1986, *Fundamentals of Cosmic Physics*, 11, 1
- Scalo, J. 1998, in *The Stellar Initial Mass Function*, ed. G. Gilmore, I. Parry, S. Ryan, Cambridge: Cambridge University Press, p. 201
- Scalo, J. 2005, in *The Initial Mass Function 50 years later*. Eds by E. Corbelli and F. Palla, *ASSL*, 327, 23
- Schilbach, E., Kharchenko, N. V., Piskunov, A. E., Röser, S., Scholz, R.-D. 2006, *A&A*, 456, 523
- Schmeja, S., Kharchenko, N. V., Piskunov, A. E., Röser, S., Schilbach, E. 2014, *A&A*, 568, 51
- Scholz, A., Geers, V., Clark, P., Jayawardhana, R., Muzic, K. 2013, *ApJ*, 775, 138
- Selman, F. J., Melnick, J. 2005, *A&A*, 443, 851
- Selman, F. J., Melnick, J. 2008, *ApJ*, 689, 8162
- Shadmehri, M. 2004, *MNRAS*, 354, 375
- Sharma, S., Pandey, A. K., Ogura, K. et al. 2008, *AJ*, 135, 1934
- Shatsky, N., Tokovinin, A. 2002, *A&A*, 382, 92
- Sung, H., Bessell, M. S. 2010, *AJ*, 140, 2070
- Vincke, K., Breslau, A., Pfalzner, S. 2015, *A&A*, 577, 115
- Weidner, C., Kroupa, P. 2004, *ApJ*, 348, 187
- Weidner, C., Kroupa, P., Pflamm-Altenburg, J. 2013, 434, 84
- Weisz, D. R., Johnson, B. D., Johnson, L. C., Skillman, E. D., Lee, R. C. et al. 2012, *ApJ*, 744, 44
- Weisz, D. R., Johnson, C. L., Foreman-Mackey, D., Dolphin, A. E., Beerman, B. F. et al. 2015, *ApJ*, 806, 198
- Zhang, Q., Fall, S. M. 1999, *ApJ*, 527, L81
- Zinnecker, H., Yorke, H. W. 2007, *ARA&A*, 45, 481

APPENDIX A: SAMPLING TECHNIQUE AND ADDITIONAL DETAILS ON THE GENERATED SAMPLES

The results presented in the main part of the paper rely on the random sampling of the masses of clusters in the initial cluster mass function (ICLMF) and on the masses of star systems in each individual cluster. Each cluster mass, M_{cl} , out of which stellar masses are randomly drawn, is itself drawn from a total mass reservoir given by $\Sigma_{cl} = \text{SFR} \times \tau_{15}$ where SFR is the assumed Galactic star formation rate and $\tau_{15} \approx 12.3$ Myrs is sum of the Hydrogen+Helium burning phases of an O star with a mass of $15 M_{\odot}$ (Ekström et al. 2012). With the values of the Galactic SFR adopted in this

work (0.68 to $1.45 \text{ M}_\odot \text{ yr}^{-1}$), this yields mass reservoirs in the range $\approx (8.3 - 17) \times 10^6 \text{ M}_\odot$. The methodology of the random sampling of cluster masses and of stellar masses is identical in nature with the exception that the probability distribution functions of the initial cluster mass function (ICLMF) is a power law function (Eq. 4), whereas the system IMF is described by the tapered-power function (Eq. 6) with a given set of parameters (γ, Γ, M_{ch}) which are themselves randomly drawn from the different families of probability distribution functions display in Figure 1.

In order to sample one mass from the ICLMF (respectively the IMF), we choose a uniform random value $M_{cl,i}$ (respectively, $M_{*,i}$) of the cluster mass (respectively, stellar mass) between the minimum and maximum mass limits assigned to each function ($M_{cl,min}$ and $M_{cl,max}$ for the ICLMF, and $M_{*,min}$ and $M_{*,max}$ for the IMF) as well as a random value Y_i using a standard random number generator. We evaluate $\text{ICLMF}(M_{cl,i})$ (respectively, $\text{IMF}(M_{*,i})$) and compare it to Y_i . If $\text{ICLMF}(M_{cl,i}) > Y_i$ (respectively, if $\text{IMF}(M_{*,i}) > Y_i$), the value of $M_{cl,i}$ (respectively, $M_{*,i}$) is admitted. Otherwise, the drawn mass is discarded and the sampling proceeds using a new value of $M_{cl,i}$ (respectively, of $M_{*,i}$). In theory, this iterative process should continue until the sum of the sampled masses is equal to Σ_{cl} (or to M_{cl} for the case of the IMF). However, the probability of the sum of sampled masses being exactly equal to the desired mass is marginal. It is therefore necessary to define a strategy for when to stop the sampling process. One method is the stop after approach, in which the sampling of new masses is stopped immediately after the iteration that causes the sampled mass to be larger than the desired mass. An alternative is to remove the last mass that is drawn. In this stop before approach, the total sampled mass is always smaller than the desired mass. As in Haas & Anders (2010), we follow a stop nearest approach in which we compare the sum of the sampled masses before and after the last iteration that causes the sum of sampled masses to go beyond the desired mass. Between these two iterations, the one that is adopted is the one that causes the sum of the sampled masses to be the nearest to the desired mass.

The total number of clusters in the ICLMF depends on the adopted Galactic SFR, the chosen slope of the ICLMF, β , and on its lower mass cutoff $M_{cl,min}$ (the upper mass cutoff is fixed in our models to $5 \times 10^4 \text{ M}_\odot$). With our adopted range of values for the SFR, β , and $M_{cl,min}$, the number of clusters in the ICLMF varies from ≈ 15000 for the cases with the lowest value of the SFR ($0.68 \text{ M}_\odot \text{ yr}^{-1}$), the lowest value of β (1.8), and the largest value of $M_{cl,min}$ (50 M_\odot), to ≈ 80000 for cases with the highest value of the SFR ($1.45 \text{ M}_\odot \text{ yr}^{-1}$), the highest value of β (2.2), and for $M_{cl,min} = 50 \text{ M}_\odot$, and up to ≈ 210000 for the highest values of the SFR ($1.45 \text{ M}_\odot \text{ yr}^{-1}$), the highest value of β (2.2), and the lowest value of $M_{cl,min}$ (10 M_\odot). It should be noted that since the quantities we are calculating ($f_{single,O}$ and $f_{lonely,O}$) are dimensionless numbers, the calculated values are insensitive to the choice of the SFR, insofar as the ICLMF is complete at the low mass end, which is the case for the values of parameters explored in this work.